ORIGINAL ARTICLE

ISSN: 2455-8095
doi: https://doi.org/10.21477/ijapsr.3.4.2

Corrosion Inhibition of Copper in 2M Nitric Acid Solution by 2-(Thiobenzyl)-5-Nitro-1H-Benzimidazole

Nagnonta Hippolyte Coulibaly[1], Yapi Serge Brou[1], Sagne Akpa[2], Juan Creus[3] and Albert Trokourey[1]

[1]Laboratoire de Chimie Physique (LCP), Université Félix Houphouet-Boignyd'Abidjan, 22 BP 582 Abidjan 22, Côte d'Ivoire.

[2]Laboratoire de Chimie Organique et Substances Naturelles (LCOSN), Université Félix Houphouët-Boigny d'Abidjan, 22 BP 582 Abidjan 22, Côte d'Ivoire.

[3]Laboratoire des Sciences de l'Ingénieur pour l'environnement (LaSIE) UMR 7356 CNRS, Université de La Rochelle, Avenue Michel Crépeau 17042 La Rochelle Cedex 1, France.

ABSTRACT

Pickling with nitric acid is commonly practiced in industry for finishing metal surfaces. The use of inhibitors during the pickling operation is of very recent origin. The TBNBI inhibition effect on copper corrosion in 2M nitric acid solution was investigated by weight loss method in relation to the temperature (25 to 40°C) and inhibitor concentration range 10^{-4} to 5.10^{-3} M. The results show that TBNBI is a good inhibitor for copper and the inhibition efficiency increases with concentration of TBNBI but decreases with increase in temperature. The adsorption parameters $(\Delta G^0_{ads}, \Delta H^0_{ads}, \Delta S^0_{ads})$ and the activation ones $(E_a, \Delta H^*_a, \Delta S^*_a)$ for the corrosion process in inhibited and uninhibited nitric acid solution were also calculated using Arrhenius equations. It can be concluded that the adsorption of the compound is spontaneous and found to occur through both physisorption and chemisorption processes. The adsorbed film on copper surface was characterized using optic microscopy and Raman spectroscopy. The surface analysis confirmed the inhibition action of TBNBI.

Quantum chemical calculations using Gaussian 09 at B3LYP level with 6-31G (d,p) basis set lead to obtain molecular descriptors such as E_{HOMO} (energy of the highest occupied molecular orbital), E_{LUMO} (energy of the lowest unoccupied molecular orbital), ΔE (energy gap) and μ (dipole moment). The global reactivity descriptors such as χ (electronegativity), η (hardness), S (softness) and ω (electrophilicity index) were derived using Koopman's theorem and analyzed. We used the condensed Fukui function and softness indices, Mulliken population analysis for local reactivity study. The calculated results are consistent with the experimental data.

Keywords: Copper; nitric acid; corrosion inhibition; mass loss technique; quantum chemical parameters; Fukui indices.

1. INTRODUCTION

Copper is a widely used material for its physical properties in many industrial applications such as fabrication of heat exchanger tubes and cooling water system due to its thermal and electrical conductivities (Zhang et al., 2014). Copper is also used in transport, telecom and oil extract. The copper material should regularly be cleaned because of the participation of carbonates or oxides which causes their thermal or electrical conductivities to be diminished. The most widely used cleaning solution contains nitric, chlorhydric, a sulfuric acid, however copper is very susceptible to corrosion in acid solutions. The corrosion problem leads to the deterioration of many metal installations. The replacement of these facilities requires enormous economic resources.The use of inhibitors (Abdallah et al., 2011) is one of the most practical method to protect metals against corrosion and preserve industrial facilities. Several heterocyclic nitrogen containing compounds were used as corrosion inhibitors for copper in acidic media (Bahrami et al., 2010; Gece, 2008; Lagrenee et al., 2002). Most of these inhibitors were aromatic and heterocyclic compounds containing nitrogen. Benzotriazole (BTA) and its derivatives were studied extensively, and BTA was proved to be a highly efficient inhibitor for preventing copper and copper-base alloys corrosion in neutral and alkaline media (Zhang et al., 2014). Unfortunately, most of these compounds are synthetic chemicals which may be very expensive, toxic and hazardous to living creatures and environ-

Corresponding author
Nagnonta Hippolyte Coulibaly
Email : coulibalynagnonta@yahoo.fr

Received: 28-08-2018 **Accepted:** 17-09-2018 **Available Online:** 01-10-2018

ment (Elhousni et al., 2017). Benzimidazole derivatives are well known because of their non-toxicity and good inhibitor efficiency in various media (Abboud et al., 2007).

Adsorption can be described by two mean types of interactions (Zhang et al., 2014): Physisorption involves electrostatic forces between ionic charges or dipoles on the adsorbed species and the electric charge at the metal/solution interface. The heat of adsorption is low, and therefore this type of adsorption is stable only at relatively low temperatures. Chemisorption involves charge sharing or charge transfer from the inhibitor molecule to the metal surface to form a coordinate type bond. In fact, electron transfer is typical for transition metals having vacant low-energy electron orbital. Chemisorption is typified by much stronger adsorption energy than physical adsorption. Such bond is therefore more stable at higher temperature.

The aim of this paper is to study the influence of a benzimidazole derivative namely 2-(thiobenzyl)-5-nitro-1H-benzimidazole ($C_{14}H_{11}N_3O_2S$) (Akpa et al., 2016) on the corrosion of copper in 2M HNO_3 solutions using experimental (weight loss method, Raman spectroscopy and optic microscopy) studies. Theoretical calculations provide an explanation of the inhibitor efficiency.

2. EXPERIMENTAL

2.1 Materials and Reagents

2.1.1 Copper samples

The copper specimens were in the form of rod measuring 10 mm in length and 2.2 mm in diameter; they were cut in commercial copper of purity 95%.

2.1.2 The tested molecule

The structure of 2-(thiobenzyl)-5-nitro-1H-benzimidazole ($C_{14}H_{11}N_3O_2S$) is given in Figure 1.

TBNBI was synthesized in the Laboratory (Akpa et al., 2016). Its molecular structure was identified by 1H NMR, 13C NMR and mass spectroscopy.

RMN ^{1}H(DMSOd-6, δ ppm): 4.63 (2H, s, SCH_2); 7.24-7.35 (3H, m, H_{ar}); 7.47-7.49 (2H, m, H_{ar}); 7.59-7.62 (1H, m, H_{ar}); 8.04-8.08 (1H, m, H_{ar}); 8.32- 8.33 (1H, m, H_{ar}).

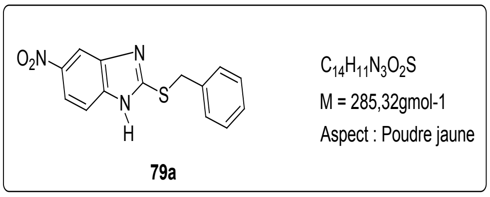

Figure 1: Chemical structure of 2-(thiobenzyl)-5-nitro-1H-benzimidazole (TBNBI)

RMN ^{13}C(DMSOd-6, δ ppm): 34.96 (S-CH_2); 110.34 (C_{ar}); 113.25 (C_{ar}), 117.46 (C_{ar}); 127.45 (C_{ar}); 128.50 (2C_{ar}); 128.91 (2C_{ar}); 137.09 (2C_{ar}); 142.13 (C_{ar}); 155.9 (N=C-S).

SDM: m/e (%) = 281.3 (10); 283 (20); 284.9 (35); 285.8 (100); 286.8 (13).

2.1.3 Solution

The aggressive solution 2M HNO_3 was prepared by dilution of analytical grade 69% nitric acid PANREAC with distilled water. Solutions of TBNBI with concentrations in the ranging from 0.1 mM to 5mM were prepared.

2.2 Weight loss measurements

The weight loss measurements were carried out in 50 mL capacity glass beaker placed in a thermostat JULABO water bath to maintain temperature. The solution volume was 50 mL.

Before measurements the copper samples were polished successively with emery paper up to 3200 grade, then rinsed thoroughly with acetone and distilled water. After drying in the drying oven at 80°C for 20 minutes the sample were accurately weighed with an analytical balance (± 0.1 mg), the copper sample was immersed in the acid solution for 1 hour. At the end of the tests, the sample were taken out, washed with distilled water, dried and reweighted accurately.In order to get good reproducibility, experiments were carried out in triplicate. The average weight loss of three parallel copper samples was obtained.

The corrosion rate (W) and inhibiton efficiency (η) were calculated from Equation 1–2 respectively:

$$w = \frac{m_1 - m_2}{s.t}\left(mgh^{-1}cm^{-2}\right) \qquad (1)$$

Where, m_1 and m_2 are respectively the weights of the sample before and after immersion (h), S is the sample surface (cm^2) and t is the immersion period (h).

$$\eta = \frac{w_1 - w_2}{w_1} \times 100\% \qquad (2)$$

In this equation, w_1 and w_2 are respectively the corrosion rates of copper after immersion of sample in the solution without and with the tested compound.

2.3. Surface analysis

2.3.1 Raman Spectroscopy

Raman spectroscopy measurements were performed using a Jobin Yvon Horiba high resolution spectrometer (LabRam HR8000 model) with a monochromatic He-Ne laser source of wavelength λ = 632.817 nm. Spectrum processing is performed using JobinYvon'sLabSpec software.

2.3.2 Optic microscopy

The morphology of the sample surface after immersion of 8 h in the 2 M HNO_3 solution with and without inhibitor was analyzed with a LEICA DM6000 M optical microscope equipped with LAS V4.9 software.

2.4 Quantum chemical studies

In order to support experimental data, theoretical calculations were carried out using Gaussian 09 W software package (Wazzan and Mahgoub, 2014). The TBNBI structure was fully and geometrically optimized (Figure 2) using density functional theory (DFT) with the functional hybrid B3LYP (Becke, three-parameter, Lee-Yang-Parr exchange-correlation function) with electron basis set 6-31G (d,p) (Udhayakala et al., 2012). The calculated quantum chemical parameters correlated to the inhibition efficiency are the frontier molecular orbital energies E_{HOMO} (highest occupied molecular orbital energy), E_{LUMO} (lowest unoccupied molecular orbital energy), energy gap (ΔE), dipole moment (μ) and other parameters including global hardness (η), global softness (S), absolute electronegativity (χ), electrophilicity index (ω) and the fraction of electrons transferred (ΔN) from the inhibitor molecule to the metal. The local reactive sites has been analyzed through the condensed Fukui function and condensed softness indices using Mulliken population analysis.

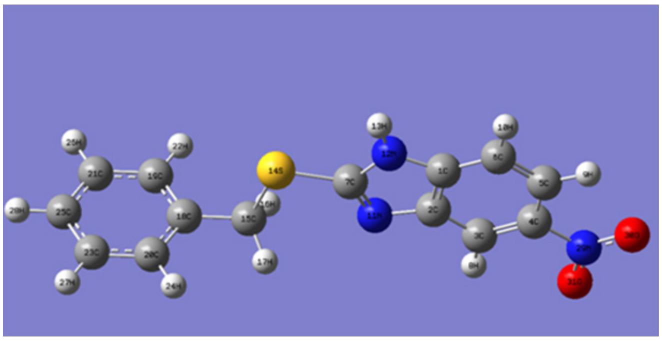

Figure 2: Optimized structure of TBNBI with labels by B3LYP/6-31G (d,p)

3. RESULTS AND DISCUSSION

3.1 Weight loss measurements

3.1.1 Corrosion rate and inhibition efficiency

The weight loss method has found broad practical application. A major advantage of this method is its relative simplicity and availability. In addition, the method uses a direct parameters for the quantitative evaluation of corrosion, the loss in mass of the metal (Niamien, 2016). The data obtained for the corrosion behaviour of copper in 2M HNO_3 solutions with and without TBNBI at different temperatures from weigth loss measurements are presented in Figure 3.

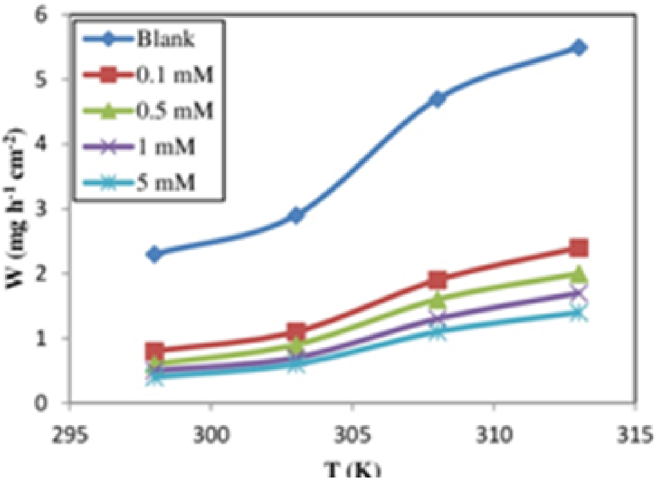

Figure 3: Evolution of corrosion rate with temperature for different concentrations of TBNBI

It is clear from figures that corrosion rate and inhibition efficiency are influenced by inhibitor concentration and system temperature.Increase in inhibitor concentration is found to decrease the corrosion rate (Figure 3) and increase the inhibition efficiency (Figure 4). The maximum inhibition efficiency of 82.6 % is afforded by 5mM of TBNBI at 298K showing that TBNBI inhibits the corrosion of copper in 2M HNO_3 solution.

It is however observed that rise in temperature leads to a decrease in inhibition efficiency (Figure 4). The decrease in inhibition efficiency with increasing temperature is suggestive of physisorption mechanism, generally attributed to electrostatic interaction between charged molecules and charged metal. This observation can be interpreted by the reduction in stability of the adsorbed film at higher temperature. According to Ay El-Etre, as temperature increases, Gibbs free energy and change in enthalpy rise to a higher value, so that some of the chemical bonds joining the molecules onto the metallic surface are impaired and the film stability reduced. It may further be attributed to a possible shift of the adsorption/desorption equilibrium towards desorption of adsorbed

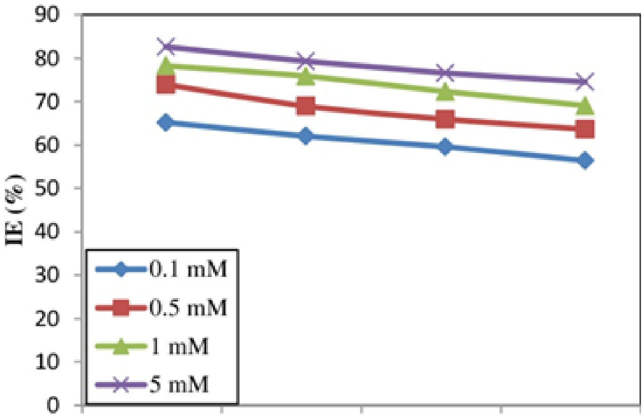

Fig. 4: Inhibition efficiency versus temperature for different concentrations

inhibitor due to increasing solution agitation. Thus, as the temperature increases the number of adsorbed molecules decreases, leading to a decrease in the inhibition efficiency (El-Etre, 2007).

3.1.2 Adsorption isotherms

It is generally accepted that organic inhibitor inhibits metal corrosion by getting adsorbed on the surface and the process is mere substitution in which water molecules on the metal surface are replaced by inhibitor molecules (Gerengi et al., 2016). Adsorption isotherms become then very important in determining the mechanism of organic electrochemical reactions. The most frequently used adsorption isotherms are Langmuir, Temkin and Frumkin (Emregül and Atakol, 2003). By far, best fit is obtained for Langmuir adsorption isotherm. Langmuir adsorption isotherm is defined by Equation 3 (Gerengi et al., 2016):

$$\frac{C_{inh}}{\theta} = \frac{1}{K_{ads}} + C_{inh} \qquad (3)$$

However, slopes present slight deviations from unity (Table 1). Therefore, the more suitable model is modified Langmuir one. The deviation of the value of slopes to unity is due to the interactions between the adsorbed species on the metal surface. The modified Langmuir model takes into account the interactions between the adsorbed species. The modified Langmuir equation is as follows (Villamil et al., 1999):

$$\frac{C_{inh}}{\theta} = \frac{n}{K'_{ads}} + nC_{inh} \qquad (4)$$

Where, n is the slope of the straight line corresponding to the Langmuir isotherm.

The curve of C_{inh}/θ as a function of C_{inh} (inhibitor concentration) is shown in Figure 5.

The values of adsorption equilibrium constant were obtained from the intercepts of the straight lines on the C_{inh}/θ -axis. is related to the standard free adsorption energy   according to Equation 5 (Lebrini et al., 2008):

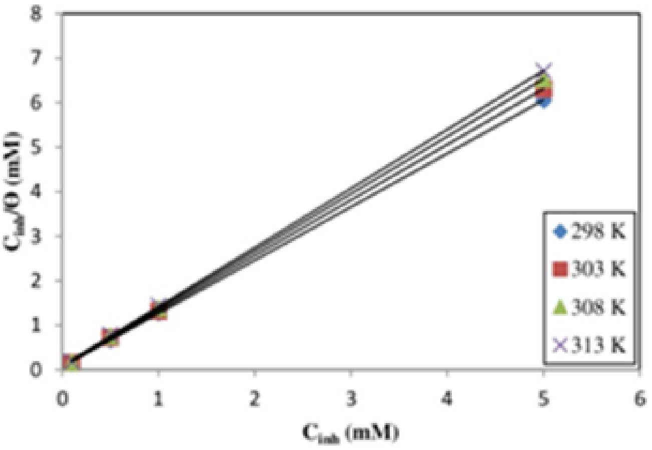

Figure 5: Langmuir isotherm for the adsorption of TBNBI on the surface of copper in 2M HNO_3

$$\Delta G^0_{ads} = -RT \ln 55.5K_{ads} \qquad (5)$$

Where, 55.5 is the concentration of water in the solution in mol. L^{-1}, R is the perfect gas constant and T is the absolute temperature.

The standard adsorption enthalpy and the standard adsorption entropy are related by the following equation:

$$\Delta G^0_{ads} = \Delta H^0_{ads} - T\Delta S^0_{ads} \qquad (6)$$

Using the obtained values of from the modified Langmuir isotherm, we can plot versus T (Figure 6). This plot gives straight line with (ΔS^0_{ads}) as slope and (ΔH^0_{ads}) as intercept.

Adsorption parameters of TBNBI tested on copper in 2M HNO3 at different temperatures are gathered in Table 1

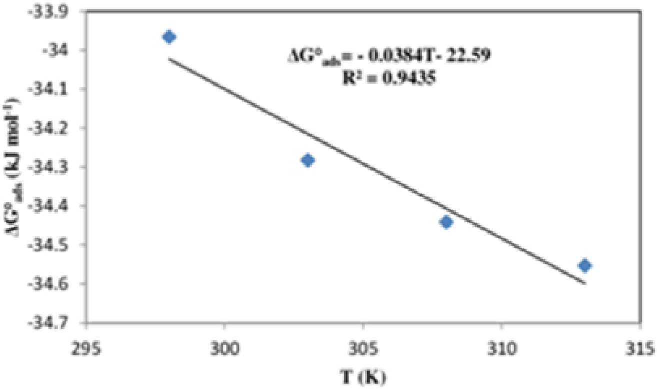

Figure 6: Free adsorption enthalpy versus temperature.

Table 1: Adsorption parameters of TBNBI tested on copper in 2 M HNO_3 at different temperatures.

T(K)	R^2	slope	Inter-cept	K_{ads} (M^{-1})	$\Delta G°_{ads}$ ($kJmol^{-1}$)	$\Delta H°_{ads}$ (kJ/mol)	$\Delta S°_{ads}$ (J/mol/K)
298	0.9999	1.1993	0.0613	16313.2	–33.97	–22.59	38.40
303	0.9999	1.2481	0.0678	14749.3	–34.28		
308	0.9999	1.2906	0.0795	12578.6	–34.44		
313	0.9998	1.3249	0.0944	10593.2	–34.55		

Values of ΔG^0_{ads} were found to be around –34 kJ mol^{-1}. It is usually accepted that the values of ΔG^0_{ads} around –20 $kJ.mol^{-1}$ or lower indicates the electrostatic attraction between the charged metal surface and charged organic molecules in the bulk of the solution. Those around –40 $kJ.mol^{-1}$ or higher involve charge sharing or charge transfer between the metal and the organic molecules. The negative value of ΔG^0_{ads} obtained reveals the spontaneity of adsorption process. In our investigation we conclude that inhibitive action of TBNBI results from both physical and chemical adsorption of its molecules on copper surface. The negative value of ΔH^0_{ads} indicates an exothermic process. It is well known in literature (El Ouali et al., 2010) that an exothermic process is associated to physisorption or chemisorption but an endothermic process signifies chemisorption. The positive value of ΔS^{0}_{ads} denote a disorder, probably due to desorption of water molecules.

3.1.3 Temperature effect

Temperature is one of the factors that can modify the behavior of materials in a given corrosive medium as well as the inhibitory efficiency of a compound. The Arrhenius dependence between the corrosion rate and the temperature allowed us to calculate the energy of activation E_a in the absence and in the presence of inhibitor using the following relation:

$$w = A\exp\left(-\frac{E_a}{RT}\right) \qquad (7)$$

The change in activation entropy and the change in activation enthalpy are obtained by applying the transition state equation:

$$\log\left(\frac{w}{T}\right) = \left[\log\left(\frac{R}{Nh}\right) + \frac{\Delta S_a}{2.300R}\right] - \frac{\Delta S_a}{2.303RT} \qquad (8)$$

Where, R (J mol^{-1}. K^{-1}) is the perfect gas constant, h (J s) the Planck constant, T (K) the absolute temperature, ℵ(mol^{-1}) the number of Avogadro and A the pre-exponential factor of Arrhenius.

Figure 7 and figure 8 show respectively the curves and $\ln w = f\left(\frac{1000}{T}\right)$.

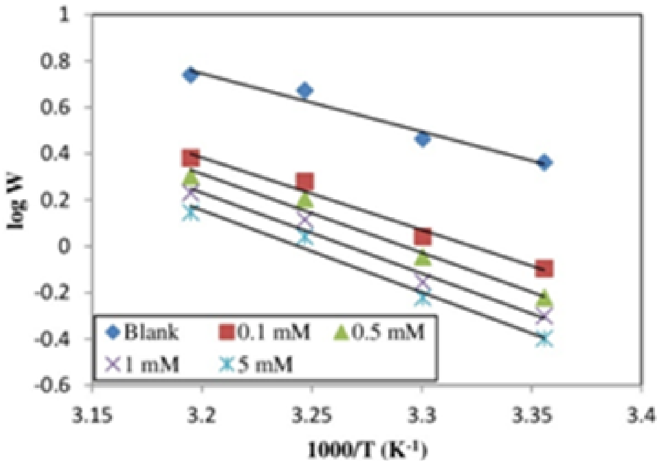

Figure7: Arrhenius plots for Copper corrosion in 2 M HNO_3 solutions without and withTBNBI

The slope of each straight line gives the value of activation energy for the blank and different concentrations of TBNBI solutions.

The slopes $\left(-\frac{\Delta H_a}{2.303R}\right)$ and the intercepts $\left[\log\left(\frac{R}{Nh}\right)+\frac{\Delta S_a}{2.303R}\right]$ are used to determine the change in activation entropy and the change in activation enthalpy. All the activation parameters are collected in Table 2.

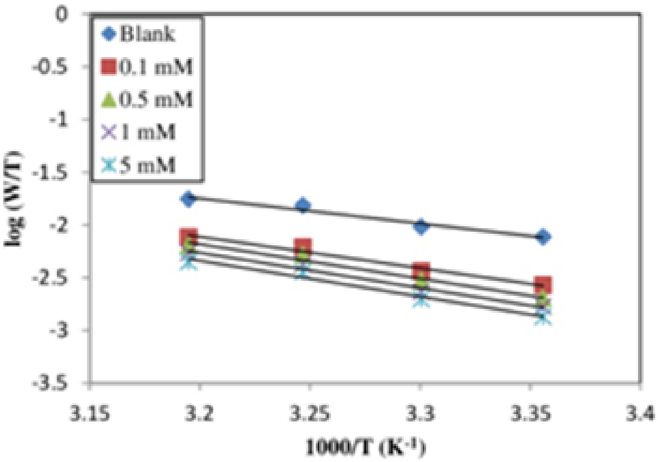

Figure 8: Transition state plots for copper corrosion in 2M HNO_3 without and with TBNBI

Table 2: Activation parameters for copper corrosion without and with TBNBI in 2M HNO_3

Concentrations	*E_a (kJ/mol)*	*(kJ/mol)*	*ΔS^{*}_{a} (J/mol/K)*
Blank	48.07	45.47	-85.14
0.1 mM	59.61	56.99	-55.20
0.5 mM	65.00	62.38	-39.30
1 mM	66.54	63.92	-35.94
5 mM	67.74	65.12	-33.55

The value of E_a for copper corrosion in free 2 M HNO_3 solution (48.07 kJ mol^{-1}) is in the same order of magnitude of some literature data for copper (Ehouman et al., 2016).Values of E_a obtained with inhibitor are higher than that for the uninhibited one, indicating a strong inhibitive action for the studied compounds by increasing the energy barrier for the corrosion process, emphasizing the electrostatic character of the inhibitor's adsorption on copper surface (El Ouali et al., 2010). The increase in activation energy can be attributed to an appreciable decrease in the adsorption of the inhibitor on the copper surface with increase in temperature. This type of inhibitor retards corrosion at ordinary temperatures but inhibition is diminished at elevated temperature.

3.2. Surface analysis

3.2.1 Raman Spectroscopy

Raman spectroscopy characterization of the copper surface after 8 hours exposure to 2 M HNO_3 solution, without or with addition of TBNBI, was performed in order to investigate the interactions of TBNBI with the copper surface. Figure 9 shows the spectra collected in addition to those of the pure TBNBI molecule in powder state. Attributions of the main bands are given in Table 3 on the basis of literature data (Furini et al., 2016; Oturak et al., 2015; Ozturk et al., 2011).

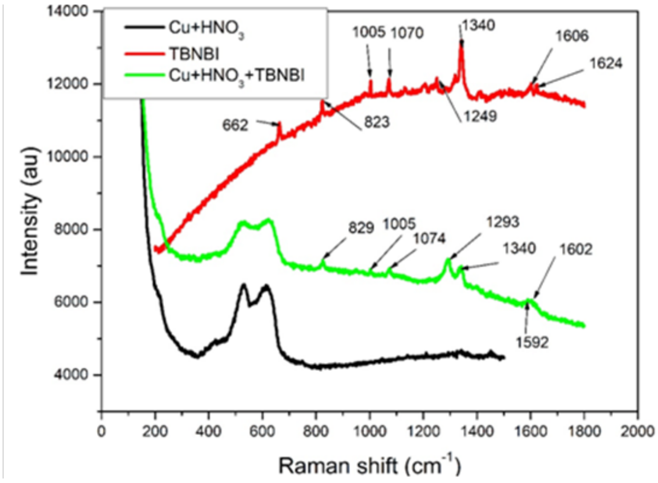

Figure 9: Raman spectra collected on the TBNBI molecule (red) and on the copper electrode after 8 h immersion in 2 M HNO_3 without (black) or with (green) 2 mM of TBNBI

When the film is formed without TBNBI, the main feature of the spectrum is a doublet at 500 and 630 cm^{-1} attributed to Cu_2O formation (Qafsaoui et al., 2016). This band still appears in the spectrum of the film formed in 2 mM TBNBI but with a weak intensity which indicates that TBNBI retards oxide formation on the copper surface. The characteristic peaks (CN, CS, NH, and CNC) in the TBNBI spectrum appear to be very weak in the SERS spectrum probably due the bindings between N,S-heteroatoms and the copper atom. This confirms the presence of a TBNBI layer on the Cu electrode.

Table 3: Vibrational wavenumbers and assignments for TBNBI molecule and surface film

TBNBI powder (cm^{-1})	*Sample TBNBI-Cu (cm^{-1})*	*Tentative assignments*
1624	1606	CC
1606	1592	CC, CH
1340	1340	CN
1249	1293	NH, in plane bending
1070	1074	CS, CC
1005	1005	CS
823	829	NH, out of plane bending
662	–	δCNC

It is acceptable to think that Cu_2O can be metastable formed on the Cu surface even at open circuit potential in nitric acid (Khaled and Al-Qahtani, 2009). The presence of Cu_2O may facilitate adsorption TBNBI via H-bond formation. The adsorption layer acts as an additional barrier to the corrosive attack and enhances the performance of the passive layer as a result (Khaled and Al-Qahtani, 2009).

3.2.2 Optic microscopy

Figures 10 (a-c) shows the Cu specimens before and after immersed in 2 M HNO_3 solution for 8 hours without and with 2 mM TBNBI at 298 K. The uninhibited copper

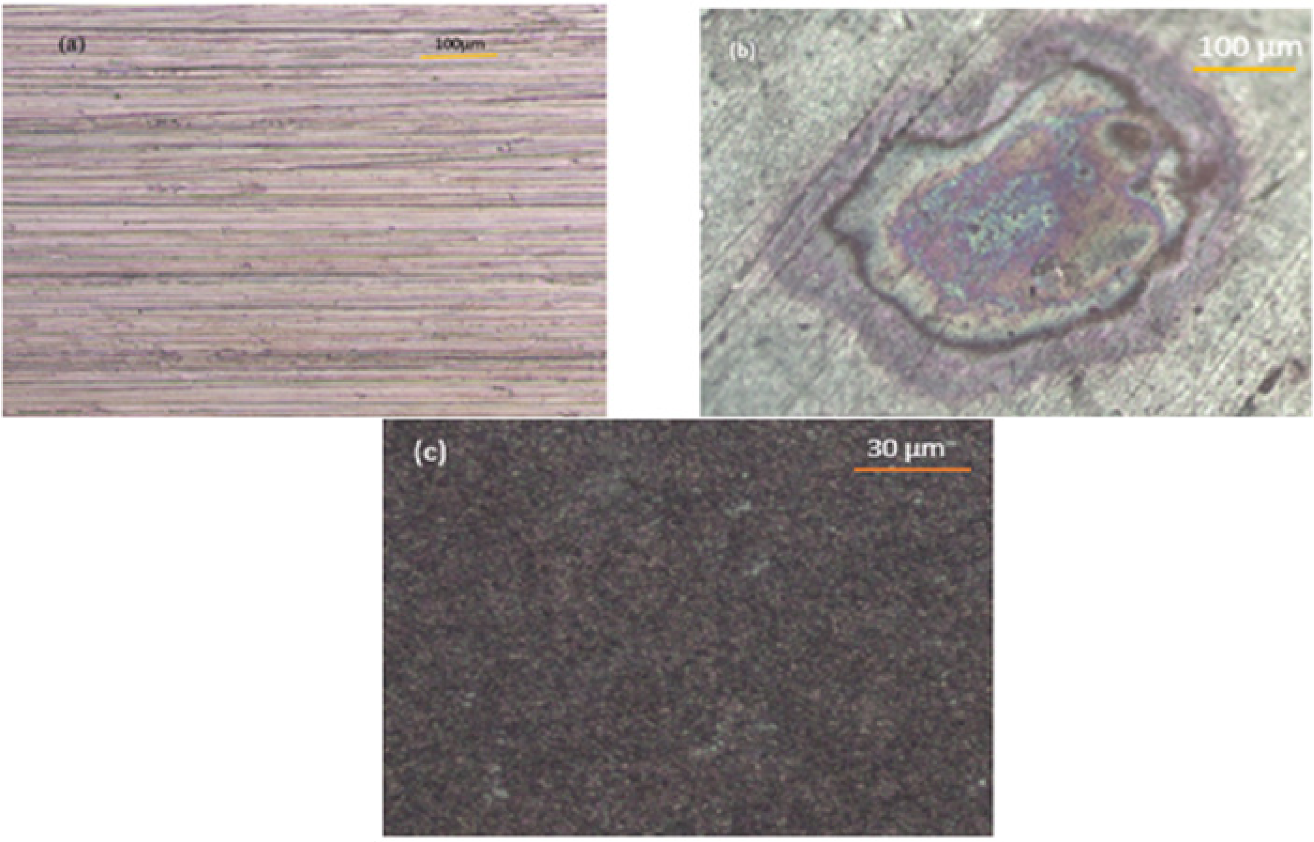

Figure 10: Pictures of the copper surface: a) freshly polished; b) after immersion in 2 M HNO_3 solution; (c) after immersion (t = 8 hours) in 2 M HNO_3 solution with 2 mM of TBNBI.

surface (Figure 10b) is severely damaged by HNO_3 corrosion and becomes rough. Figure 10c indicates that the copper surface seems to be almost not affected by corrosion and is smoother than corroded one. It is obvious that corrosive attack is considerably restricted by passive layer of TBNBI and oxidized surface (Cu_2O) species.

3.3 Quantum chemical Calculations

Quantum chemical calculations were carried out to study the mechanism of adsorption and inhibition of the molecule studied in functional theory of density by the hybrid functional B3LYP (Becke 3 parameters Lee Yang Parr) with the base of orbitals 6-31G (d, p) using the Gaussian 09W software.

3.3.1 Global Parameters

This theoretical study of the TBNBI molecule has been carried out with a view to highlighting the factors which may favor its inhibitory nature. The calculated chemical parameters include the energy of the highest occupied (E_{HOMO}) and lowest unoccupied (E_{LUMO}) molecular orbital, the energy difference $\Delta E = E_{LUMO}-E_{HOMO}$, the dipole moment (μ) and the charges of Mulliken on heteroatoms. Parameters such as ionization potential (I), electronic affinity (A), electronegativity (χ), global hardness (η), global softness (S), global electrophilicity index (ω), fraction of transferred electrons (ΔN) and total energy change (ΔE_T) were also calculated using the following relationships (Niamien et al., 2012):

$$I = -E_{HOMO} \quad (9)$$

$$A = -E_{LUMO} \quad (10)$$

$$\chi = \frac{1}{2}(I + A) \quad (11)$$

$$\eta = \frac{1}{2}(I - A) \quad (12)$$

$$S = \frac{1}{\eta} = \frac{2}{I - A} \quad (13)$$

$$w = \frac{\mu_p^2}{2\eta} = \frac{\chi^2}{2\eta} \quad (14)$$

$$\Delta N = \frac{\chi_{Cu} - \chi_{inh}}{2(\eta_{Cu} + \eta_{inh})} \quad (15)$$

Where, χ_{Cu} and χ_{inh} denote respectively the absolute electronegativity of copper and the inhibitor, η_{Cu} and η_{inh} are respectively the global hardness of copper and the inhibitor. In this work ΔN has been determined using theoretical value of $\chi_{Cu} = 4.98$ eV (Pearson, 1986) and $\eta_{Cu} = 0$ (El Ibrahimi et al., 2016).

Figure 11 shows Mulliken charges distribution of TBNBI molecule obtained with DFT at the B3LYP/6-31G (d,p) level of theory in water solution phase. There is a general consensus by several authors that the more negatively charged an atom is, the more it can be adsorbed on the metal surface through donor-acceptor type reaction(Li et al., 2007; Özcan et al., 2004).It can therefore be easily seen that the oxygen, nitrogen, sulfur and carbon atoms of the benzene ring carry a high density of negative charges and could therefore constitute active adsorption sites.

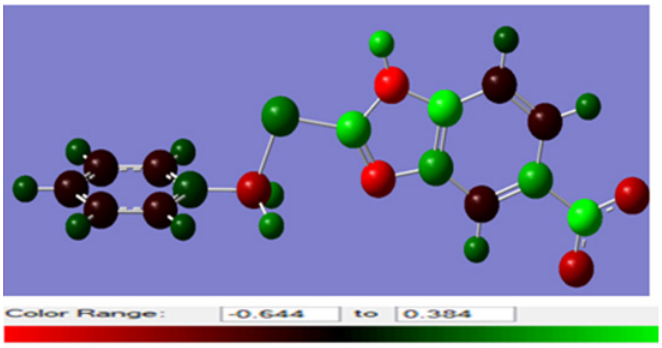

Figure 11: Mulliken charges distribution of TBNBI.

Analyzing HOMO-LUMO diagrams (Figure 12), we can observe that HOMO and LUMO densities are concentrated in nearly the same region, around the following atoms: oxygen, nitrogen and carbon atoms of the benzimidazole ring, indicating that they are potential active centers for donor-acceptor interactions. The corrosion inhibition action of the molecule can be achieved via these adsorption centers (Martinez and Štagljar, 2003).

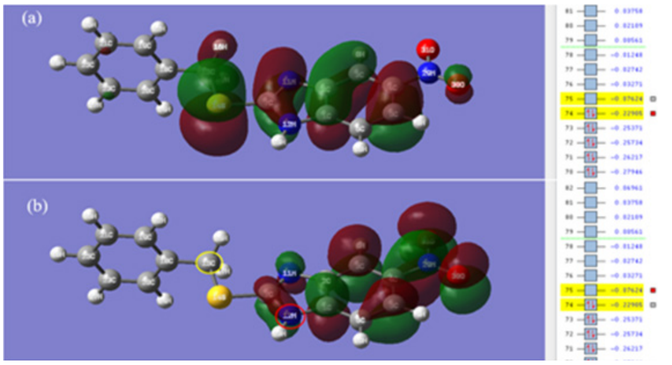

Figure 12: HOMO (a) and LUMO (b) Diagrams of TBNBI using B3LYP/6-31G (d, p)

HOMO energy is often associated with the ability of a molecule to give electrons, while LUMO energy indicates its ability to accept electrons. The binding capacity of the inhibitor to the metal surface (Popova et al., 2003) increases with increasing the HOMO value and decreasing the LUMO energy value. The quantitative parameters of quantum chemistry and reactivity are collected in Table 4. The energy gap ($\Delta E = E_{LUMO}-E_{HOMO}$) is

Table 4: Quantum chemical descriptors for TBNBI

Parameters	*Values*	*Parameters*	*Values*
EHOMO(eV)	–6.2328	A(eV)	2.0746
ELUMO(eV)	–2.0746	χ(eV)	4.1537
ΔE(eV)	4.1582	ΔN	0.1987
μ(D)	7.4000	η(eV)	2.0791
I(eV)	6.2328	S(eV)	0.4809
W(eV)	4.1492	ΔE_T(eV)	–0.5197

an important parameter as a function of reactivity of the inhibitor molecule towards the adsorption on the metallic surface. Lower values of the energy gap will render good inhibition efficiency, because the energy to remove an electron from the last occupied orbital will be low. In our case, the low value of 4.1582 eV when compared with that of many good inhibitors in the literature could explain the good inhibition efficiency of TBNBI (Jeeva et al., 2017).

It is known that the value of the dipole moment (μ) characteristic of the hydrophobicity of the molecule decreases when the efficiency of the inhibition increases, suggesting that the molecules whose dipole moment is weak will easily adsorb to the metal surface. Similar results can be found in the literature, although several authors state that the inhibitory efficiency increases with the increasing values of the dipole moment. In fact, a literature review (Khaled et al., 2005) reveals several irregularities in the case of the correlation between the dipole moment and the inhibitory efficiency. In general, there is no significant relationship between the value of the dipole moment and the inhibitory power of a molecule.

Global hardness (η) and softness (S) are important molecular properties to measure molecular reactivity and selectivity. Generally, a huge energy gap is observed for a hard molecule and a small energy gap is observed for a soft molecule. Hence, the reactivity of soft molecules is higher than that of hard molecules because they could easily donate electrons to an acceptor. Based on the computed values of hardness (2.0791 eV) and softness (0.4809 $(eV)^{-1}$) (Table 4) we can say that TBNBI has small hardness and high softness values compared with many molecules in the literature (Kouakou et al., 2016; Niamien et al., 2012).

The absolute electrophilicity index was also calculated. According to the definition, this index measures the propensity of chemical species to accept electrons. A high value of electrophilicity index (Parr et al., 1999) describes a good electrophile while a small value of electrophilicity index denotes a good nucleophile. This reactivity index measures the stabilization in energy when the system acquires an additional electronic charge from the environment. In this work the obtained value (ω = 4.1492) shows the good capacity of TBNBI to donate electrons.

Negative sign of total energy change (ΔE_T= - 0.5197 eV) shows that the charge transfer to the molecule followed by back-donation from the molecule is energetically favorable (charge transfer to the molecule and back-donation from the molecule). Similar observation has been reported in the literature (Niamien et al., 2012).

The parameter ΔN, the number of electrons transferred, also known as the ability to exchange electrons, indicates the tendency of a molecule to give electrons to the metal surface if $\Delta N > 0$ and the opposite if $\Delta N < 0$ (PetrovićMihajlović et al., 2017). In our case the obtained value of ΔN (0.1987) shows that the inhibition efficiency results from electron donation.

3.3.2 Local Parameters

Prediction of local selectivity such as condensed Fukui functions $\left[f\left(\vec{r}\right)\right]$ and condensed local softness $\left[s\left(\vec{r}\right)\right]$ indices can provide a chemical insight into atoms that have a significant tendency toward donation or acceptance of whole or fraction of electrons (Obot et al., 2015). In this method the chemical reactivity of inhibitors can be evaluated for each atom. The nucleophilic $\left(\left(f_k^+\right)\right)$ and electrophilic $\left(\left(f_k^-\right)\right)$ Fukui functions can be calculated using the finite difference approximation as follows (Jeeva et al., 2017):

$$f_k^+ = q_k(N+1) - q_k(N) \quad (16)$$

$$f_k^- = q_k(N) - q_k(N-1) \quad (17)$$

Where, q_k represents the atomic charge of atom k. $q_k(N+1)$, $q_k(N)$ and $(q_k(N-1)$ and are the charges of the atoms on the systems with (N + 1), N, and (N – 1) electrons, respectively.

Condensed softness indices ($s^{\pm}$) of the molecules can be calculated from the following relation between global softness (s) and condensed Fukui function ($f^{\pm}$) (Kouakou et al., 2016).

$$s_k^+ = f_k^+ \times S \quad (18)$$

$$s_k^- = f_k^- \times S \quad (19)$$

The values of the Fukui functions for a nucleophilic $\left(f_k^+\right)$ and electrophilic $\left(f_k^-\right)$ attack are given for TNBI in Table 5 for non-hydrogen atoms.

The preferred site for nucleophilic attack is the atom in the molecule where the value of is maximum and it is associated with the LUMO region while the site for electrophilic attack is controlled by the values of which is associated with the HOMO region. In TBNBI, the highest value was found at N(12) atom with 0.039949 indicating

Table 5: Condensed Fukui function and local softness values of TBNBI.

Atome	q(N+1)	q(N)	q(N-1)	f_k^+	f_k^-	s_k^+	s_k^+
1C	0.319366	0.350208	0.372052	-0.030842	-0.021844	-0.01483192	-0.01050478
2C	0.208500	0.20477	0.229446	0.00373	-0.024676	0.00179376	-0.01186669
3C	-0.179317	-0.121674	-0.078271	-0.057643	-0.043403	-0.02772052	-0.0208725
4C	0.259843	0.234214	0.239794	0.025629	-0.00558	0.01232499	-0.00268342
5C	-0.119635	-0.117432	-0.082187	-0.002203	-0.035245	-0.00105942	-0.01694932
6C	-0.129498	-0.107644	-0.085223	-0.021854	-0.022421	-0.01050959	-0.01078226
7C	0.221665	0.293594	0.301589	-0.071929	-0.007995	-0.03459066	-0.0038448
11N	-0.534415	-0.532831	-0.49506	-0.001584	-0.037771	-0.00076175	-0.01816407
12N	-0.603618	-0.643567	-0.62351	0.039949	-0.020057	0.01921147	-0.00964541
14S	0.003138	0.161668	0.365871	-0.15853	-0.204203	-0.07623708	-0.09820122
15C	-0.385736	-0.38298	-0.436924	-0.002756	0.053944	-0.00132536	0.02594167
18C	0.118078	0.083961	0.106253	0.034117	-0.022292	0.01640687	-0.01072022
19C	-0.112584	-0.101617	-0.098157	-0.010967	-0.00346	-0.00527403	-0.00166391
20C	-0.112506	-0.101619	-0.099951	-0.010887	-0.001668	-0.00523556	-0.00080214
21C	-0.086646	-0.084901	-0.076133	-0.001745	-0.008768	-0.00083917	-0.00421653
23C	-0.086381	-0.084902	-0.074005	-0.001479	-0.010897	-0.00071125	-0.00524037
25C	-0.100133	-0.081812	-0.064456	-0.018321	-0.017356	-0.00881057	-0.0083465
29N	0.288008	0.384345	0.410237	-0.096337	-0.025892	-0.04632846	-0.01245146
30O	-0.529361	-0.407859	-0.365071	-0.121502	-0.042788	-0.05843031	-0.02057675
31O	-0.508913	-0.399757	-0.362289	-0.109156	-0.037468	-0.05249312	-0.01801836

that N(12) is the preferred site for nucleophilic attack and the atom C(15) is the preferred site for electrophilic attack since this atom has the highest value of Fukui function (0.053944).

4. CONCLUSION

2-(thiobenzyl)-5-nitro-1H-benzimidazole (TBNBI) was found to be an efficient inhibitor for the corrosion of copper in 2M nitric acid. The inhibition efficiency was increased with inhibitor concentration and attributed to physisorption of TBNBI molecules on the metal surface since the values of Ea in the solution with inhibitor are higher than that in blank solution. The Langmuir adsorption isotherm exhibited the best fit to the experimental data. The negative sign of and indicate that the adsorption process of TBNBI is spontaneous and exothermic. The positive of can be attributed to the increase in the solvent entropy and more positive water desorption entropy. The optic micrographs and Raman spectroscopy showed that the inhibitor molecules form with oxidized surface (Cu_2O) species a good protective film onto the copper surface. The quantum chemical method shows that TBNBI molecules can be adsorbed at the copper surface on the basis of donor-acceptor interactions between the π-electrons of benzene ring, N atoms and metal atoms.

5. REFERENCES

1. Abboud Y, Abourriche A, Saffaj T, Berrada M, Charrouf M, et al., (2007). 2, 3-Quinoxalinedione as a novel corrosion inhibitor for mild steel in 1M HCl. Materials chemistry and physics. 105:1-5.
2. Abdallah M, Atwa ST, Abd-Allah N, Fouda A (2011). Azole derivatives as inhibitors for the corrosion of irradiated and non-irradiated carbon steel in HNO3 solution. Anti-Corrosion Methods and Materials. 58:31-38.
3. Akpa SJ, Zoakouma RSP, Say VM, Ouattara M, Kone MW, Sissouma D, Adjou A, (2016). Synthesis and in vitro antifungal evaluation of 2-thioalkylaryl-benzimidazoles derivatives against Candida albicans. International Journal of Biological and Chemical Sciences. 10:1403-1412.
4. Bahrami M, Hosseini S, Pilvar P (2010). Experimental and theoretical investigation of organic compounds as inhibitors for mild steel corrosion in sulfuric acid medium. Corrosion science. 52:2793-2803.
5. Ehouman D, Akpa, J, Niamien P, Sissouma D, Trokourey A (2016). Copper corrosion inhibition by 2-thiobenzylbenzothiazole in 2M nitric acid. Der Pharma Chemica. 88(10):274-286.
6. El-Etre, A (2007). Inhibition of acid corrosion of carbon steel using aqueous extract of olive leaves. Journal of Colloid and Interface Science. 314:578-583.
7. El Ibrahimi B, Soumoue A, Jmiai A, Bourzi H, et al., (2016). Computational study of some triazole derivatives (un-and protonated forms) and their copper complexes in corrosion inhibition process. Journal of Molecular Structure. 1125: 93-102.
8. El Ouali I, Hammouti B, Aouniti A, Ramli Y, et al., (2010). Thermodynamic characterisation of steel corrosion in HCl in the presence of 2-phenylthieno (3, 2-b) quinoxaline. J. Mater. Environ. Sci. 1:1-8.
9. Elhousni L, Galai M, ElKamraoui FZ, Dkhireche N, Touir R, EbnTouhami M (2017). Corrosion and scale studies of copper used in Moroccan industrial cooling water systems.

Euro-Mediterranean Journal for Environmental Integration. 2:12.

10. Emregül KC, Atakol O (2003). Corrosion inhibition of mild steel with Schiff base compounds in 1 M HCl. Materials chemistry and physics. 82:188-193.
11. Furini L, Constantino C, Sanchez-Cortes S, Otero J, López-Tocón I (2016). Adsorption of carbendazim pesticide on plasmonic nanoparticles studied by surface-enhanced Raman scattering. Journal of colloid and interface science. 465:183-189.
12. Gece G (2008). The use of quantum chemical methods in corrosion inhibitor studies. Corrosion science. 50:2981-2992.
13. Gerengi H, Ugras HI, Solomon MM, Umoren SA, Kurtay M, Atar N (2016). Synergistic corrosion inhibition effect of 1-ethyl-1-methylpyrrolidinium tetrafluoroborate and iodide ions for low carbon steel in HCl solution. Journal of adhesion science and Technology. 30:2383-2403.
14. Jeeva M, Prabhu GV, Rajesh C, (2017). Inhibition effect of nicotinamide and its Mannich base derivatives on mild steel corrosion in HCl. Journal of Materials Science. 52:12861-12888.
15. Khaled K, Al-Qahtani M (2009). The inhibitive effect of some tetrazole derivatives towards Al corrosion in acid solution: Chemical, electrochemical and theoretical studies. Materials Chemistry and Physics. 113:150-158.
16. Khaled K, Babić-Samardžija K, Hackerman N (2005). Theoretical study of the structural effects of polymethylene amines on corrosion inhibition of iron in acid solutions. Electrochimica Acta. 50:2515-2520.
17. Kouakou V, Niamien PM, Yapo AJ, Diaby S, Trokourey A (2016). Experimental and DFT Studies on the Behavior of Caffeine as Effective Corrosion Inhibitor of Copper in 1M HNO3. Orbital-The Electronic Journal of Chemistry. 8:66-79.
18. Lagrenee M, Mernari B, Bouanis M, Traisnel M, Bentiss F (2002). Study of the mechanism and inhibiting efficiency of 3, 5-bis (4-methylthiophenyl)-4H-1, 2, 4-triazole on mild steel corrosion in acidic media. Corrosion Science. 44:573-588.
19. Lebrini M, Traisnel M, Lagrenée M, Mernari B, Bentiss F (2008). Inhibitive properties, adsorption and a theoretical study of 3, 5-bis (n-pyridyl)-4-amino-1, 2, 4-triazoles as corrosion inhibitors for mild steel in perchloric acid. Corrosion Science. 50:473-479.
20. Li W, He Q, Pei C, Hou B (2007). Experimental and theoretical investigation of the adsorption behaviour of new triazole derivatives as inhibitors for mild steel corrosion in acid media. Electrochimica Acta. 52:6386-6394.
21. Martinez S, Štagljar I (2003). Correlation between the molecular structure and the corrosion inhibition efficiency of chestnut tannin in acidic solutions. Journal of Molecular Structure: THEOCHEM. 640:167-174.
22. Niamien P, Kouakou V, Yapo A, Diaby S, Trokourey A (2016). Copper Corrosion Inhibition in 1 M Nitric Acid. Adsorption and Inhibitive Action of Theophylline. Chem Sci Rev Lett: 5(20):131-146
23. Niamien P, Kouassi H, Trokourey A, Essy F, Sissouma D, Bokra Y (2012). Copper Corrosion Inhibition in 1 M HNO3 by Two Benzimidazole Derivatives. ISRN Materials Science. 2012:1-15.
24. Obot I, Macdonald D, Gasem Z (2015). Density functional theory (DFT) as a powerful tool for designing new organic corrosion inhibitors. Part 1: an overview. Corrosion Science. 99:1-30.
25. Oturak H, Kinaytürk NK, Şahın G (2015). Structure and Vibrational Studies of □ 1-(1H-Benzoimidazol-2-YL) Ethanol, Using DFT Method. Acta Physica Polonica A.128: B417-B421.
26. Özcan M, Dehri I, Erbil M (2004). Organic sulphur-containing compounds as corrosion inhibitors for mild steel in acidic media: correlation between inhibition efficiency and chemical structure. Applied surface science. 236:155-164.
27. Ozturk I, Kourkoumelis N, Hadjikakou S, Manos M, et al., (2011). Interaction of antimony (III) chloride with thiourea, 2-mercapto-5-methyl-benzimidazole, 3-methyl-2-mercaptobenzothiazole, 2-mercaptopyrimidine, and 2-mercaptopyridine. Journal of Coordination Chemistry. 64:3859-3871.
28. Parr RG, Szentpaly Lv, Liu S (1999). Electrophilicity index. Journal of the American Chemical Society. 121:1922-1924.
29. Pearson RG (1986). Absolute electronegativity and hardness correlated with molecular orbital theory. Proceedings of the National Academy of Sciences. 83:8440-8441.
30. PetrovićMihajlović MB, Radovanović MB, Tasić ŽZ, Antonijević MM (2017). Imidazole based compounds as copper corrosion inhibitors in seawater. Journal of Molecular Liquids. 225:127-136.
31. Popova A, Christov M, Deligeorgiev T (2003). Influence of the molecular structure on the inhibitor properties of benzimidazole derivatives on mild steel corrosion in 1 M hydrochloric acid. Corrosion. 59:756-764.
32. Qafsaoui W, Kendig MW, Joiret S, Perrot H, Takenouti H, (2016). Ammonium pyrrolidine dithiocarbamate adsorption on copper surface in neutral chloride media. Corrosion Science. 106: 96-107.
33. Udhayakala P, Rajendiran T, Gunasekaran S (2012). Theoretical Evaluation of Corrosion Inhibition Performance of Some Triazole Derivatives. Journal of Advanced Scientific Research. 3.
34. Villamil RF, Corio P, Agostinho SM, Rubim JC (1999). Effect of sodium dodecylsulfate on copper corrosion in sulfuric acid media in the absence and presence of benzotriazole. Journal of Electroanalytical chemistry. 472:112-119.
35. Wazzan NA, Mahgoub FM (2014). DFT calculations for corrosion inhibition of ferrous alloys by pyrazolopyrimidine derivatives. Open Journal of Physical Chemistry. 4:6.
36. Zhang X, Wallinder IO, Leygraf C (2014). Mechanistic studies of corrosion product flaking on copper and copper-based alloys in marine environments. Corrosion Science. 85:15-25.

How to cite article: Nagnonta Hippolyte Coulibaly, Yapi Serge Brou, Sagne Akpa, Juan Creus and Albert Trokourey (2018). Corrosion Inhibition of Copper in 2M Nitric Acid Solution by 2-(Thiobenzyl)-5-Nitro-1H-Benzimidazole. Int. J. Appl. Pharm. Sci. Res. 3(4):54-63. doi: https://doi.org/10.21477/ijapsr.3.4.2

Source of Support; Nil **Conflict of Interest:** None declared